On investigation of kink-solitons and rogue waves to a new integrable (3+1)-dimensional KdV-type generalized equation in nonlinear sciences

Brij Mohan* Sachin Kumar[†] Raj Kumar[‡]

*Department of Mathematics, Hansraj College, University of Delhi, Delhi -110007, India †Department of Mathematics, Faculty of Mathematical Sciences, University of Delhi, Delhi 110007, India ‡Department of Mathematics, Kirorimal College, University of Delhi, Delhi-110007, India

Abstract: This research study proposes a novel (3+1)-dimensional Painlevé integrable KdV-type equation that generalizes well-known equations in soliton theory and nonlinear sciences. It illustrates the Painlevé analysis to establish the complete integrability of the proposed equation. We employ the Cole-Hopf transformations to get the bilinear equation in an auxiliary function and further construct it into Hirota's bilinear form. Utilizing the Hirota bilinear technique, we obtain the soliton solutions of kink types and their interactions up to the third order. It examines the rogue waves of the higher order using a direct symbolic approach up to the third order. For constructing the rogue waves, we transform the investigated equation from (3+1)-dimensional to a (1+1)-dimensional partial differential equation and form its Hirota bilinear form in transformed variables. It demonstrates the dynamics for the obtained kink-soliton and rogue wave solutions with appropriate parameter values using the symbolic system *Mathematica*. The interaction solutions of rogue waves show the dominating nature of more giant waves over smaller waves. We analyze the rogue dynamics in both the transformed and original variables. Solitons as solitary waves and rogue waves as extreme or monster waves are alluring concepts in various fields of nonlinear sciences, including oceanography, optical fibers, plasma physics, dynamical systems, and engineering.

Keywords: Bilinear form; Painlevé analysis; Interaction solutions; Hirota bilinear technique; Direct symbolic approach.

1 Introduction

In soliton theory and nonlinear sciences, solitons [1–7] have attracted researchers and scientists as a fascinating wave phenomenon. Having an equilibrium between dispersion and nonlinearity, they are distinguished by their ability to preserve their form and stability across vast distances. Solitons are essential for high-speed fiber optic communication systems called optical solitons or soliton pulses. By adjusting for the material's nonlinearity and the medium's dispersion, soliton transmission over extended distances can occur without significant distortion. This feature is necessary for reliable and efficient data transport in optical communication networks. Dispersive solitary waves or solitons are helpful in wave energy conversion, oceanography, and coastal engineering. Understanding and controlling these solitons can help to prevent coastal erosion, enhance wave prediction, and maximize wave energy extraction. The combination of the plasma's dispersive

^{*}brijmohan6414@gmail.com

[†]sachinambariya@gmail.com (Corresponding author)

 $^{^{\}ddagger}rajkmc@gmail.com$

properties and the nonlinearity caused by particle interactions results in these solitons. They are helpful in many areas of plasma physics study, including fusion investigations, plasma heating, and wave propagation in magnetized plasma. Solitons are essential to understand and use in various domains, from optical communication and high-speed data transfer to coastal management and quantum technology development.

Localized substantial solitary waves in space-time, often known as rogue waves [8–14], possess a significant amplitude. These unpredictable waves have the potential to harm humans seriously. The evolution of rogue waves is a topic of great interest to many experts from different fields of nonlinear sciences. Rogues are more significant than the surrounding waves, making them noticeable due to their unusually high height. Nonlinear science studies rogue waves due to its contradiction of models for linear waves. The research on rogue waves predicts their occurrence and understands their underlying physics. The singularity in rogue wave solutions is a critical feature of their dynamics. Singularities occur when wave amplitudes theoretically approach infinity within finite time, corresponding to extreme and sudden amplification. This behavior is often linked to constructive interference among wave components and the inherent nonlinearity of the system, leading to "wave focusing." Techniques such as Painlevé analysis are applied to the governing equations to analyze these singularities. Such tools help to identify the locations and conditions under which singularities arise, offering insights into the mechanisms behind rogue wave formation. Phase shifts and arbitrary parameters in the solutions of nonlinear PDEs shape the structure and behavior of rogue waves; such solutions are called singular-like solutions. Adjusting these parameters allows us to simulate how energy concentrates into singular points, influencing rogue waves' peak height and transiency. Researchers observe similar phenomena by understanding these dynamics, essential for practical applications ranging from oceanography and meteorology to optics and quantum mechanics.

The improvement of maritime safety is one significant usage. One can use prediction models or algorithms to provide earlier observation and awareness systems to prevent harm caused by rogue waves. The maritime sector, gas or oil outlets, and infrastructure near the coast could all benefit from knowing this information. Therefore, we may attain greater functional security and affordable solutions by comprehending the dynamical analysis of building safe structures and designing strategies to reduce the impact of rogues. The study of solitons and rogue waves has garnered significant attention in recent decades due to their fascinating properties and broad applications in oceanography, optical fibers, plasma physics, and engineering fields. Various soliton equations, such as the (1+1)-dimensional Korteweg-de Vries (KdV) and the (2+1)-dimensional Kadomtsev-Petviashvili (KP) equations, have been widely explored for their ability to model nonlinear wave phenomena. However, these lower-dimensional systems often need to capture the complexities of higher-dimensional dynamics in real-world applications. Moreover, while many methods exist to verify the integrability and solvability of soliton equations, higher-order soliton and rogue wave interactions remain under explored, particularly in high-dimensional settings, and still need to be explored. Furthermore, studies on rogue wave dynamics contribute to our understanding of problematic situations, interactions of waves, and the emergence of more significant occurrences in several nonlinear phenomena.

In this research, we propose and investigate an (3+1)-D KdV-type generalized nonlinear equation as

$$u_{xxxy} + \alpha_1 u_{yt} + \alpha_2 (u_x u_y)_x + \alpha_3 u_{xx} + \alpha_4 u_{zz} = 0, \tag{1}$$

where $\alpha_{i=1,2,3,4}$ are as real parameters, and generalizes well-known equations:

- (3+1)-D Hirota bilinear equation [15] with $\alpha_1 = -1, \alpha_2 = 3, \alpha_3 = 0, \alpha_4 = -3$

$$u_{xxxy} - u_{yt} + 3(u_x u_y)_x - 3u_{zz} = 0, (2)$$

- (3+1)-D Jimbo-Miwa equation [16] with $\alpha_1=2,\alpha_2=3,\alpha_3=0,\alpha_4=-3$

$$u_{xxxy} + 2u_{yt} + 3(u_x u_y)_x - 3u_{zz} = 0, (3)$$

- (2+1)-D BLMP equation [17] with $\alpha_1 = 1, \alpha_2 = -3, \alpha_3 = \alpha_4 = 0$

$$u_{xxxy} + u_{yt} - 3(u_x u_y)_x = 0, (4)$$

- (2+1)-D KP equation [18] under the transformation $y\to x, z\to y, u_x\to u$ with $\alpha_1=1, \alpha_2=6, \alpha_3=0, \alpha_4=\pm 3$

$$(u_t + 6uu_x + u_{xxx})_x \pm 3u_{yy} = 0, (5)$$

- (1+1)-D KdV equation [19] under the transformation $y \to x, z \to x, u_x \to u$ with $\alpha_1 = 1, \alpha_2 = 6, \alpha_3 = \alpha_4 = 0$

$$u_t + 6uu_x + u_{xxx} = 0, (6)$$

Localized solutions, including soliton, lump, breather, and others, are carried by the integrable evolution equation in specific directions. Analyzing the integrability of the nonlinear PDEs might result in exact and analytical solutions. The Painlevé test [20–22] can be used to verify the complete integrability of a nonlinear PDE. Finding out if a PDE can pass the test of Painlevé analysis gets somewhat tedious. However, symbolic systems make this investigation possible, like the system software Mathematica and Matlab. We look for particular explanations to understand the peculiarities of several facts accurately in various disciplines of nonlinear science. As mentioned previously, NLPDE has drawn the attention of several scholars to its ability to provide a wide range of solutions and closely simulate real-world scenarios. The dynamic analysis of rogue wave behavior resulting from nonlinear PDEs has made it an attractive research field for highlighting basic principles in water engineering, plasma, nonlinear sciences, and shallow water waves. Compared to existing literature, this work stands out by extending the dimension of the equation and offering a new approach to analyzing rogue wave interactions. While previous studies have mainly focused on lower-dimensional soliton solutions and first-order rogue waves, this research pushes the boundaries by considering higher-dimensional systems and providing third-order solutions. The symbolic computations carried out using Mathematica further enhance the precision and applicability of the solutions, making this method both efficient and effective for studying complex nonlinear wave phenomena. This efficiency and effectiveness make the method practical for current research and suggest its potential for further exploration and application in other nonlinear systems.

Nonlinear PDEs [23–31] deals with nonlinear functions used as models for complicated physical systems in various scientific domains. They are challenging to examine since no general analysis technique exists. Usually, each equation needs to be examined independently as a problem. Nonetheless, there are some circumstances in which broad approaches are appropriate. These techniques discretize the problem into a smaller grid after which they estimate the solution using mathematical procedures. Several methods are being used to obtain the analytic and exact solutions, such as the Darboux transformation [32–34]; the simplified Hirota's technique [35, 36]; the Bäcklund transformation [37, 38]; the Bilinear Neural Network Method [39, 40]; Lie symmetry analysis [41–43]; the Hirota's bilinearization technique [44–47]; and others.

The manuscript is structured as follows: The following section investigates the Painlevé integrability of the proposed KdV-type nonlinear equation. In Section 3, we construct Hirota's bilinear form using the Cole-Hopf transformation and obtain the soliton solutions up to third order and depict the dynamics of the these solutions. Section 4 constructs the rogue wave solutions utilizing a direct symbolic approach with the bilinear form of the equation in transformed variables. It finds the rogue waves up to the third order and plots the dynamical structures for the obtained rogue solutions. In Section 5, we discuss the findings concerning the dynamic behaviors of the shown graphics, and the last section concludes the remarks of our work and highlight its future scope.

2 Integrability: Painlevé Analysis

A reliable method for analyzing the integrability of nonlinear PDEs is the Painlevé test. The primary goal of this analysis is to find movable singularity-free solutions for a nonlinear PDE. If a PDE passes the Painlevé test, it is considered P-integrable, indicating that complex structures can be solved using specialized functions. By verifying integrable conditions, Weiss et al. [48] provided the Painlev'e test to assess the integrability of the nonlinear PDEs. Three steps make up this analysis: first, it looks at the leading-order analysis; second, it finds the resonances; and third, it verifies the resonance conditions completely. If the simple poles of the solutions correspond to all moveable singularities, then the test is considered P-integrable. The field u is expanded by Laurent's series about the singular manifold g = 0 of an analytical function g as

$$u = \sum_{\lambda=0}^{\infty} u_{\lambda} g^{\lambda+\Lambda},\tag{7}$$

where Λ and u_{λ} ; are integer and arbitrary functions, respectively. On substitution of equation (7) in (1), with leading order analysis, we get

$$\Lambda = -1$$
,

with

$$u_0 = \frac{6g_x}{\alpha_2}$$
.

It gets the resonances as

$$\lambda = -1, 1, 4, 6.$$

The resonance $\lambda = -1$ shows the arbitrary choice for singular manifold g = 0. The analysis finds the functions u_{λ} explicitly for $\lambda = 0, 2, 3, 5$ and as arbitrary for positive resonances. The positive resonances satisfied the compatibility conditions. Thus, the investigated KdV-type equation is Painlevé integrable.

3 Bilinear form and N-soliton solutions

We take Φ_i as the phase in the Eq. (1) as

$$\Phi_i = p_i x + q_i y + r_i z - w_i t, \tag{8}$$

with w_i as dispersions and p_i, q_i, r_i real parameters. Putting $u = e^{\Phi_i}$ into equation (1) for linear terms, we get the dispersion as

$$w_i = \frac{\alpha_3 p_i^2 + p_i^3 q_i + \alpha_4 r_i^2}{\alpha_1 q_i}. (9)$$

Considering the Cole-Hopf transformation of auxiliary function f as

$$u = P(\log f)_x,\tag{10}$$

and puting with $f(U,V) = 1 + e^{\Phi_1}$ and equation (9) into equation (1). On solving for P, we get

$$P = \frac{6}{\alpha_2}.$$

Now, we can transform the equation (1) with Eq. (10) in f as

$$ff_{xxxy} - 3f_x f_{xxy} + 3f_{xx} f_{xy} - f_{xxx} f_y + \alpha_1 (ff_{yt} - f_t f_y) + \alpha_3 (ff_{xx} - f_x^2) + \alpha_4 (ff_{zz} - f_z^2) = 0 \quad (11)$$

that is a bilinear equation and can be shown in Hirota's bilinear form. Hirota [19] designed the differential operators D_k : k = x, y, z, t as

$$D_x^{r_1} D_y^{r_2} D_z^{r_3} D_t^{r_4} U(x, y, z, t) V(x, y, z, t) =$$

$$\left(\frac{\partial}{\partial_x} - \frac{\partial}{\partial_{x'}} \right)^{r_1} \left(\frac{\partial}{\partial_y} - \frac{\partial}{\partial_{y'}} \right)^{r_2} \left(\frac{\partial}{\partial_z} - \frac{\partial}{\partial_{z'}} \right)^{r_3} \left(\frac{\partial}{\partial_t} - \frac{\partial}{\partial_{t'}} \right)^{r_4} U(x,y,z,t) V(x',y',z',t') |_{x=x',y=y',z=z',t=t'},$$

with x', y', z', t' as formal variables and and $r_i : 1 \le i \le 4$ as the positive integers. Thus, the equation (11) has its Hirota's bilinear form as

$$\left[D_x^3 D_y + \alpha_1 D_y D_t + \alpha_3 D_x^2 + \alpha_4 D_z^2 \right] f. f = 0.$$
 (12)

We obtain the N-soliton solution by considering an expression for the function f in closed-form given by Hirota as

$$f = \sum_{\eta=0,1} \exp\left(\sum_{i=1}^{N} \eta_i \Phi_i + \sum_{1=i (13)$$

where $\sum_{n=0,1}$ indicates the summation of all possible combinations for $\eta_i = 0, 1$ for $1 \le i \le N$.

3.1 Single kink-soliton

For N=1 in equation (13), we have $\eta_1=0$ and 1 so we take f as

$$f = f_1 = 1 + e^{\Phi_1} = 1 + e^{p_1 x + q_1 y + r_1 z - w_1 t},$$
(14)

which satisfied the equation (12). Thus, on substituting (14) with its derivative in the equation (10), we get 1-soliton solution

$$u = u_1 = \frac{6p_1 e^{p_1 x + q_1 y + r_1 z}}{\alpha_2 \left(\exp\left(\frac{t(\alpha_3 p_1^2 + p_1^3 q_1 + \alpha_4 r_1^2)}{\alpha_1 q_1}\right) + e^{p_1 x + q_1 y + r_1 z}\right)},$$
(15)

3.2 Two kink-solitons

Having N=2 in the equation (13), we have $\eta_1=\eta_2=0,1$. So there will be four combinations of $\{\eta_1,\eta_2\}$ as (0,0),(0,1),(1,0) and (1,1), therefore, the function f is

$$f = f_2 = 1 + e^{\Phi_1} + e^{\Phi_2} + e^{A_{12} + \Phi_1 + \Phi_2} = 1 + e^{\Phi_1} + e^{\Phi_2} + a_{12}e^{\Phi_1 + \Phi_2}, \tag{16}$$

where $a_{12} = e^{A_{12}}$.

On substituting the equation (16) into Eq. (12), we get

$$a_{12} = \frac{p_1^2 q_2 (\alpha_3 q_2 - 3p_2 q_1 (q_1 - q_2)) + p_2 p_1 q_1 q_2 (3p_2 (q_1 - q_2) - 2\alpha_3) + \alpha_3 p_2^2 q_1^2 + \alpha_4 (q_2 r_1 - q_1 r_2)^2}{p_1^2 q_2 (\alpha_3 q_2 - 3p_2 q_1 (q_1 + q_2)) - p_2 p_1 q_1 q_2 (3p_2 (q_1 + q_2) + 2\alpha_3) + \alpha_3 p_2^2 q_1^2 + \alpha_4 (q_2 r_1 - q_1 r_2)^2}$$
(17)

Thus, by putting Eq. (16) with (17) into (10), gives a 2-soliton solution for Eq. (1) as

$$u = u_2 = \frac{6}{\alpha_2} (\log f_2)_x \tag{18}$$

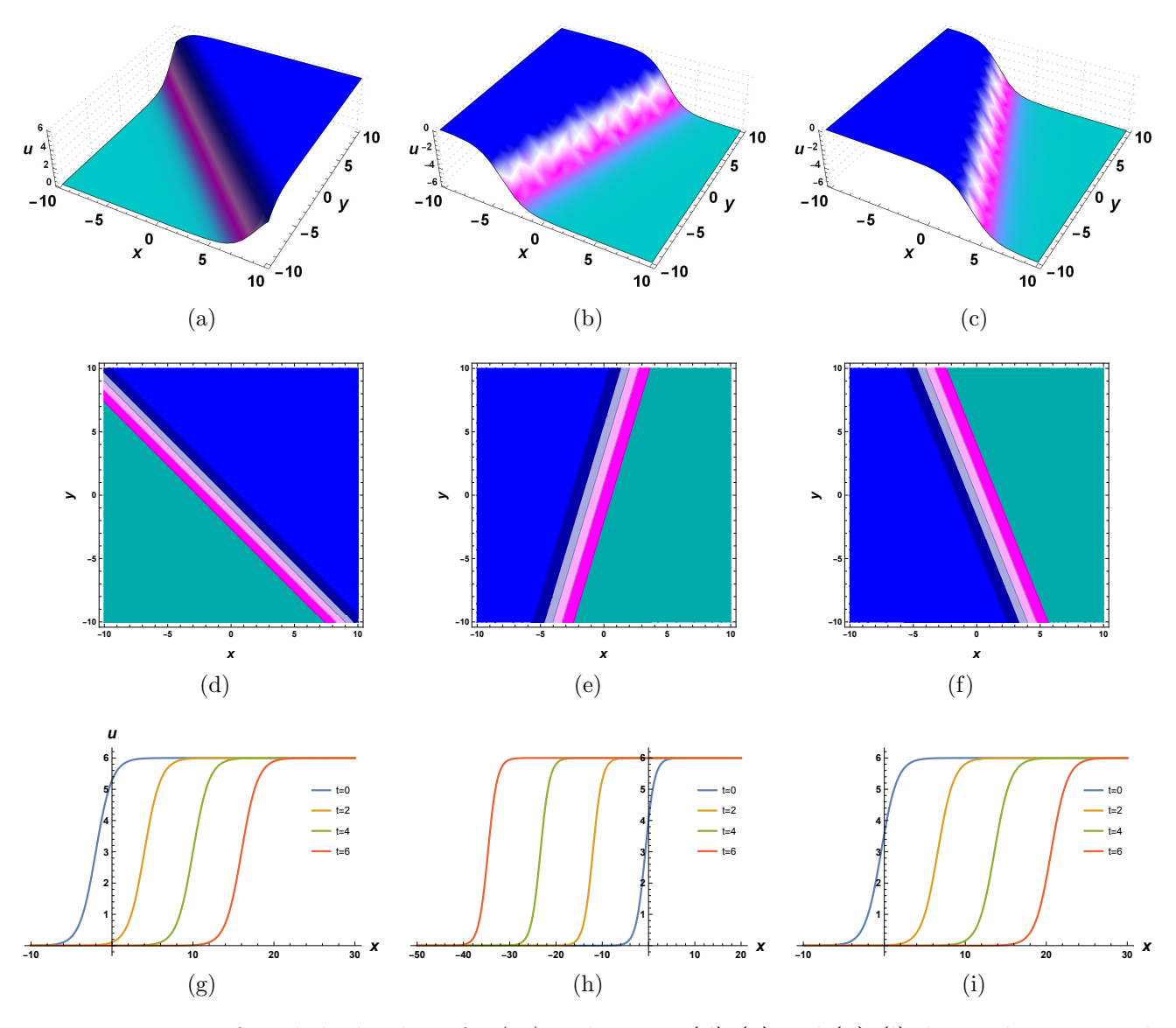


Figure 1: Dynamics of single kink-soliton for (15) with z = 0. (d)-(e) and (g)-(i) depict the contour plots in xy-plane and 2D plots at different time t, respectively.

3.3 Three kink-solitons

For N = 3 in Eq. (13), we have $\eta_1, \eta_2, \eta_3 = 0, 1$ so the total combinations for $\{\eta_1, \eta_2, \eta_3\}$ will be eight as $\{(0,0,0), (0,0,1), (0,1,0), (0,1,1), (1,0,0), (1,0,1), (1,1,0), (1,1,1)\}$, therefore, the function f is as

$$f = f_3 = 1 + e^{\Phi_1} + e^{\Phi_2} + e^{\Phi_3} + a_{12}e^{\Phi_1 + \Phi_2} + a_{13}e^{\Phi_1 + \Phi_3} + a_{23}e^{\Phi_2 + \Phi_3} + b_{123}e^{\Phi_1 + \Phi_2 + \Phi_3},$$
(19)

where $a_{ij} = e^{A_{ij}}$ and $b_{123} = e^{A_{12} + A_{13} + A_{23}} = a_{12} + a_{13} + a_{23}$. The equation (17) can be generalized as

$$a_{ij} = \frac{p_i^2 q_j (\alpha_3 q_j - 3q_i p_j (q_i - q_j)) + p_i q_i p_j q_j (3p_j (q_i - q_j) - 2\alpha_3) + \alpha_3 q_i^2 p_j^2 + \alpha_4 (r_i q_j - q_i r_j)^2}{p_i^2 q_j (\alpha_3 q_j - 3q_i p_j (q_i + q_j)) - p_i q_i p_j q_j (3p_j (q_i + q_j) + 2\alpha_3) + \alpha_3 q_i^2 p_j^2 + \alpha_4 (r_i q_j - q_i r_j)^2},$$
(20)

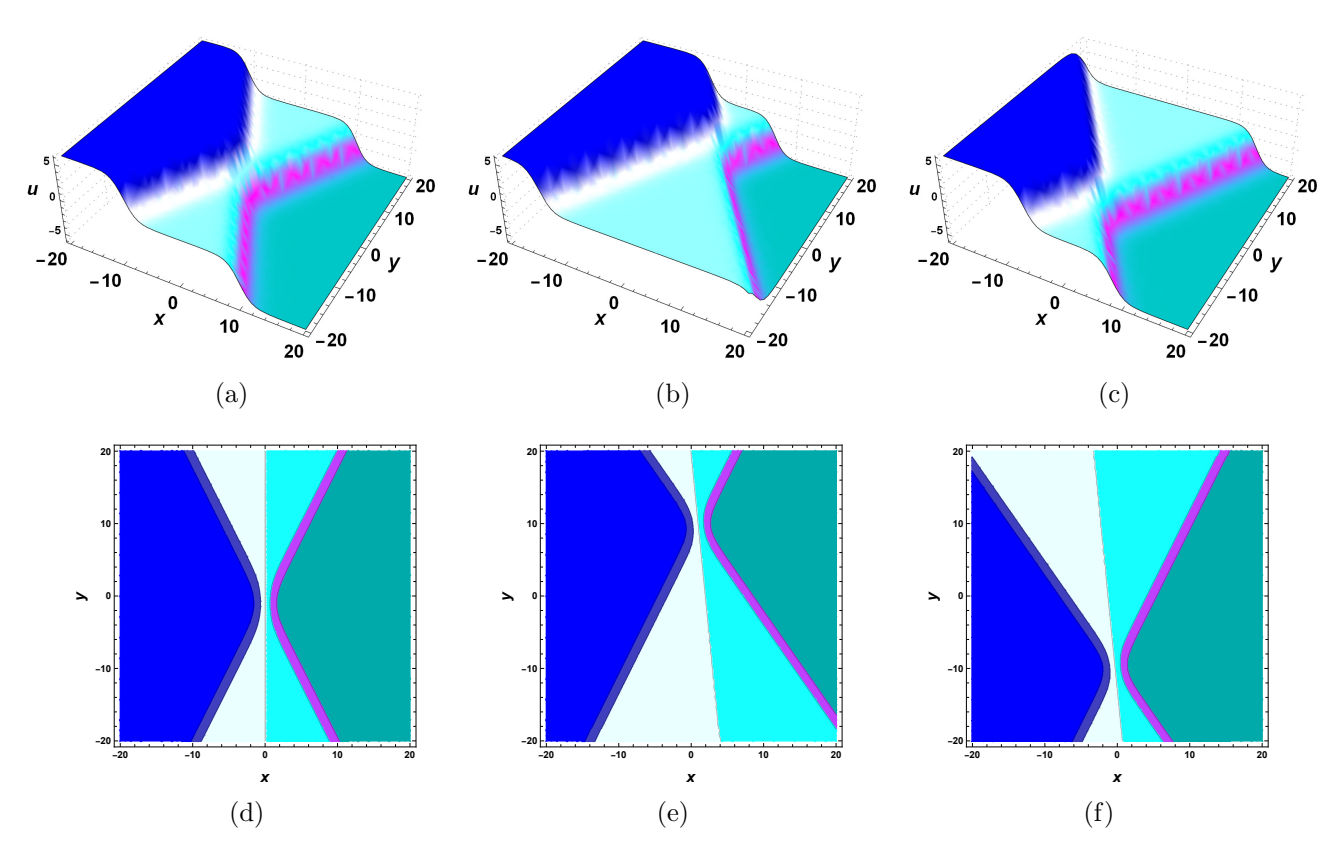


Figure 2: Dynamics of two kink-solitons for (18) with z = 0. (d)-(e) depicts the contour plots for (a)-(c) in xy-plane.

for the auxiliary function $f = 1 + e^{\Phi_1} + e^{\Phi_2} + a_{ij}e^{\Phi_1 + \Phi_2}$; 1 = i < j = 3. By substituting the Eq. (19) with (20) into the Eq. (10), we obtain the 3-soliton solution as

$$u = u_3 = \frac{6}{\alpha_2} (\log f_3)_x \tag{21}$$

4 Bilinear form and rogue waves

We consider the transformations $u = u(\xi, \eta)$ with $\xi = x + t$ and $\eta = y + z$ in equation (1). Thus, we get transformed equation as

$$\alpha_2 u_\eta u_{\xi\xi} + \alpha_4 u_{\eta\eta} + \alpha_2 u_{\xi} u_{\xi\eta} + \alpha_1 u_{\xi\eta} + \alpha_3 u_{\xi\xi} + u_{\xi\xi\xi\eta} = 0. \tag{22}$$

Taking the phase Φ_i in equation (22)

$$\Phi_i = p_i \xi - w_i \eta, \tag{23}$$

having w_i as dispersions and p_i as real-parameter. Putting $u(\xi, \eta) = e^{\Phi_i}$ into the Eq. (22), with linear terms, get

$$w_i = \frac{\alpha_1 p_i + p_i^3 \pm p_i \sqrt{\alpha_1^2 - 4\alpha_3 \alpha_4 + 2\alpha_1 p_i^2 + p_i^4}}{2\alpha_4}.$$
 (24)

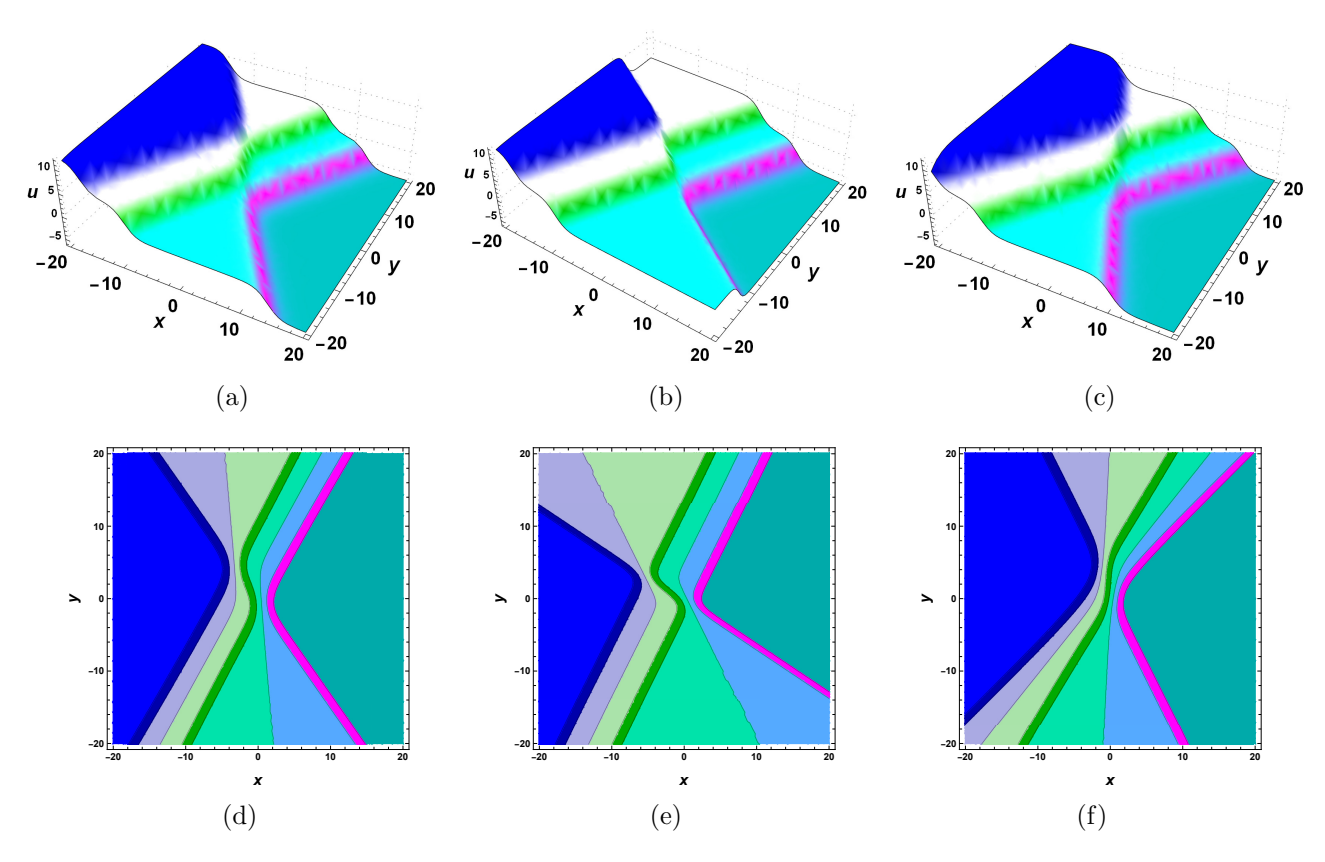


Figure 3: Dynamics of three kink-solitons for (21) with z = 0. (d)-(e) depicts the contour plots for (a)-(c) in xy-plane.

Considering the logarithmic transformation

$$u(\xi, \eta) = P(\log f)_{\xi},\tag{25}$$

with P as constant and f as auxiliary function. Putting the transformation (25) with $f(\xi, \eta) = 1 + e^{\Phi_1}$ into equation (22) gives

$$P = \frac{6}{\alpha_2}.$$

So, the transformation (25) gives a billinear equation in f of the equation (22) as

$$ff_{\xi\xi\xi\eta} - 3f_{\xi}f_{\xi\xi\eta} + 3f_{\xi\eta}f_{\xi\xi} - f_{\eta}f_{\xi\xi\xi} + \alpha_1(ff_{\xi\eta} - f_{\eta}f_{\xi}) + \alpha_3(ff_{\xi\xi} - f_{\xi}^2) + \alpha_4(ff_{\eta\eta} - f_{\eta}^2) = 0.$$
 (26)

Using Hirota's differential operators $D_i : i = \xi, \eta$

$$D_{\xi}^{n_1} D_{\eta}^{n_2} f(\xi, \eta) g(\xi, \eta) = \left(\frac{\partial}{\partial_{\xi}} - \frac{\partial}{\partial_{\xi'}} \right)^{n_1} \left(\frac{\partial}{\partial_{\eta}} - \frac{\partial}{\partial_{\eta'}} \right)^{n_2} f(\xi, \eta) g(\xi', \eta') |_{\xi = \xi', \eta = \eta'},$$

with ξ', η' as formal variables and and $n_i : i = 1, 2$ as positive integers, the equation (26) has its Hirota's bilinear form as

$$\left[D_{\xi}^{3} D_{\eta} + \alpha_{1} D_{\xi} D_{\eta} + \alpha_{3} D_{\xi}^{2} + \alpha_{4} D_{\eta}^{2}\right] f.f = 0, \tag{27}$$

which shows the similar pattern for *D*-operators to the bilinear equation (12) in original variables x, y, z, t. We obtain the rogue waves solutions by considering the function f [49,50] as

$$f(\xi,\eta) = \sum_{k=0}^{\frac{n(n+1)}{2}} \sum_{j=0}^{k} c_{n(n+1)-2k,2j} \xi^{n(n+1)-2k} \eta^{2j},$$
(28)

where n and $c_{r,s}$; $r,s \in \{0,2,\cdots,k(k+1)\}$ are positive integer and the constants, respectively.

4.1 First-order rogue waves

For n=1 in equation (28), we take auxiliary function $f(\xi,\eta)$ as

$$f = f_1 = c_{2,0}\xi^2 + c_{0,2}\eta^2 + c_{0,0}. (29)$$

On having equation (29) into the equation (27), and equating zero the coefficients of distinct powers of $\xi^r \eta^s$; $r, s \in \mathbb{Z}$, we obtain a system of equations

$$2\alpha_4 c_{0,0} c_{0,2} + 2\alpha_3 c_{0,0} c_{2,0} = 0,$$

$$2\alpha_4 c_{0,2} c_{2,0} - 2\alpha_3 c_{2,0}^2 = 0,$$

$$2\alpha_3 c_{0,2} c_{2,0} - 2\alpha_4 c_{0,2}^2 = 0.$$
(30)

On solving above system, we get parameter values as

$$c_{0,0} = 0, \quad c_{0,2} = \frac{\alpha_4 c_{0,2}}{\alpha_3}, \quad c_{2,0} = c_{2,0}.$$
 (31)

Thus, the function f in (29) becomes

$$f = f_1 = c_{0,2} \left(\frac{\alpha_4 \xi^2}{\alpha_3} + \eta^2 \right). \tag{32}$$

On substituting the equation (32) into (25), we get a solution of 1^{st} -order rogue waves as

$$u(\xi, \eta) = u_1 = \frac{12\alpha_4 \xi}{\alpha_2 (\alpha_3 \eta^2 + \alpha_4 \xi^2)}.$$
 (33)

4.2 Second-order rogue waves

For 2^{nd} -order rogue waves, we take f for n=2 in equation (28) as

$$f = f_2 = c_{6,0}\xi^6 + c_{4,2}\xi^4\eta^2 + c_{4,0}\xi^4 + c_{2,4}\xi^2\eta^4 + c_{2,2}\xi^2\eta^2 + c_{2,0}\xi^2 + c_{0,6}\eta^6 + c_{0,4}\eta^4 + c_{0,2}\eta^2 + c_{0,0}.$$
(34)

Substituting Eq. (34) into the Eq. (27), and equating zero the coefficients of distinct powers of $\xi^r \eta^s$; $r, s \in \mathbb{Z}$, gives a system. On solving the system, we get values

$$c_{0,0} = \frac{29\alpha_4 c_{4,2}}{2\alpha_1^3 \alpha_3}, \quad c_{0,2} = \frac{231c_{4,2}}{4\alpha_1^2}, \quad c_{0,4} = \frac{5\alpha_3 c_{4,2}}{\alpha_1 \alpha_4}, \quad c_{0,6} = \frac{\alpha_3^2 c_{4,2}}{3\alpha_4^2},$$

$$c_{2,0} = -\frac{9\alpha_4 c_{4,2}}{4\alpha_1^2 \alpha_3}, \quad c_{2,2} = \frac{12c_{4,2}}{\alpha_1}, \quad c_{2,4} = \frac{\alpha_3 c_{4,2}}{\alpha_4}, \quad c_{4,0} = -\frac{\alpha_4 c_{4,2}}{\alpha_1 \alpha_3}, \quad c_{4,2} = c_{4,2}$$

$$c_{6,0} = \frac{\alpha_4 c_{4,2}}{3\alpha_3}.$$

$$(35)$$

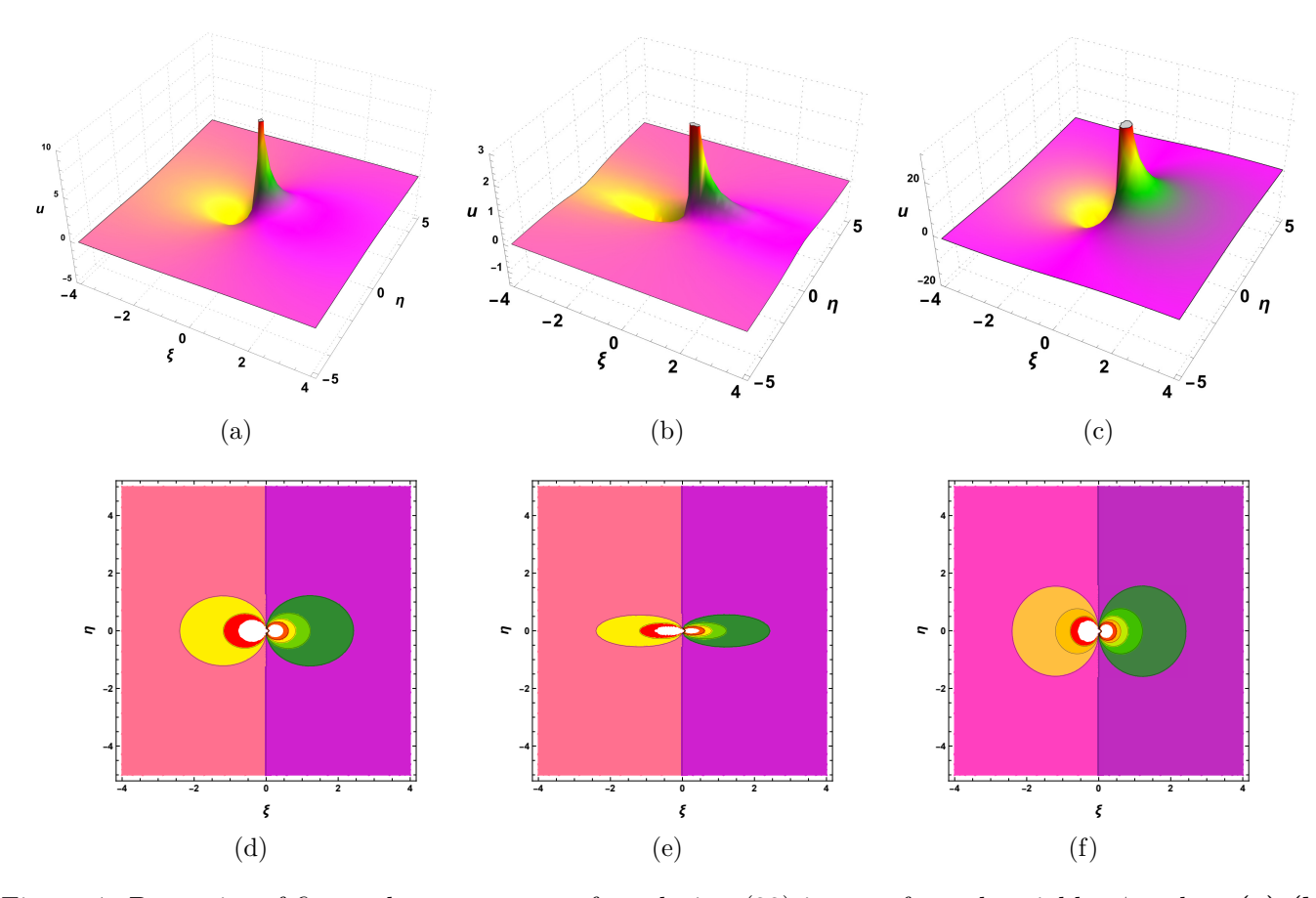


Figure 4: Dynamics of first-order rogue waves for solution (33) in transformed variables ξ and η . (a)-(b) depicts the 3D profiles in $\xi\eta$ -plane, and (d)-(f) shows the contour plots for the (a)-(c).

Thus, the function f in (34) becomes

$$f = f_2 = \frac{c_{4,2}}{12} \left(\frac{12\alpha_3 \eta^4 \xi^2}{\alpha_4} + \frac{144\eta^2 \xi^2}{\alpha_1} + \frac{4\alpha_3^2 \eta^6}{\alpha_4^2} + \frac{60\alpha_3 \eta^4}{\alpha_1 \alpha_4} + \frac{693\eta^2}{\alpha_1^2} + \frac{4\alpha_4 \xi^6}{\alpha_3} - \frac{12\alpha_4 \xi^4}{\alpha_1 \alpha_3} - \frac{27\alpha_4 \xi^2}{\alpha_1^2 \alpha_3} + \frac{174\alpha_4}{\alpha_1^3 \alpha_3} + 12\eta^2 \xi^4 \right). \quad (36)$$

On putting equation (36) into (25), we get a solution for 2^{nd} -order rogue waves as

$$u(\xi,\eta) = u_2 = \frac{36\xi \left(\frac{4\alpha_3\eta^4}{\alpha_4} + \frac{48\eta^2}{\alpha_1} - \frac{8\alpha_4\xi^2}{\alpha_1\alpha_3} + \frac{4\alpha_4\xi^4}{\alpha_3} - \frac{9\alpha_4}{\alpha_1^2\alpha_3} + 8\eta^2\xi^2\right)}{\alpha_2 \left(\frac{12\alpha_3\eta^4\xi^2}{\alpha_4} + \frac{144\eta^2\xi^2}{\alpha_1} + \frac{4\alpha_3^2\eta^6}{\alpha_1^2} + \frac{60\alpha_3\eta^4}{\alpha_1\alpha_4} + \frac{693\eta^2}{\alpha_1^2} + \frac{4\alpha_4\xi^6}{\alpha_3} - \frac{12\alpha_4\xi^4}{\alpha_1\alpha_3} - \frac{27\alpha_4\xi^2}{\alpha_1^2\alpha_3} + \frac{174\alpha_4}{\alpha_1^3\alpha_3} + 12\eta^2\xi^4\right)}.$$
(37)

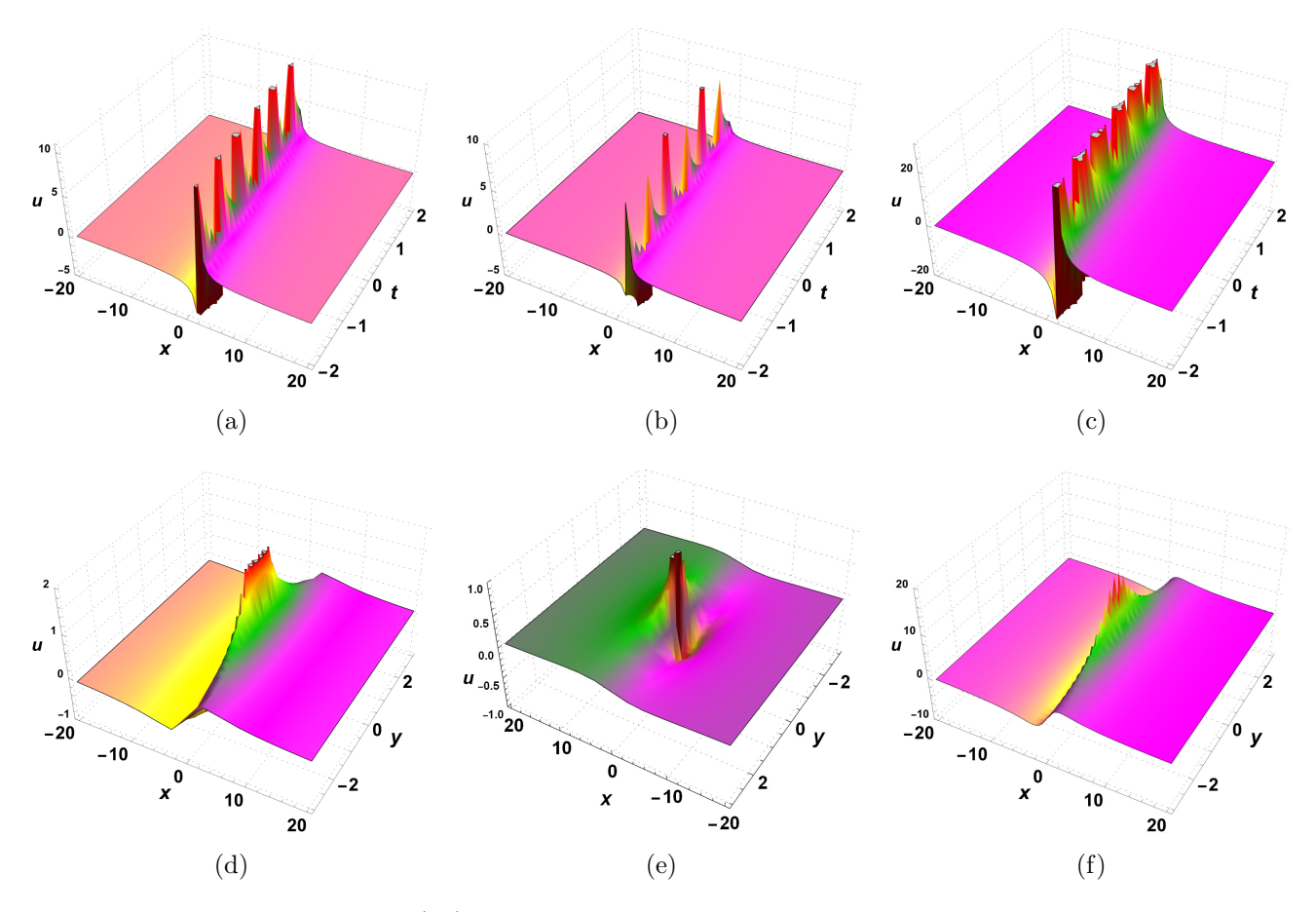


Figure 5: Dynamical profiles of (33) in the starting variables x, y, z, and t under transformed variables $\xi = x + t$ and $\eta = y + z$. (a)-(c) and (d)-(f) depict 3D profiles in xt and xy-planes, respectively.

4.3 Third-order rogue waves

Take n=3 in equation (28), we get auxiliary function f as

$$f = f_{3} = c_{12,0}\xi^{12} + c_{10,2}\xi^{10}\eta^{2} + c_{10,0}\xi^{10} + c_{8,4}\xi^{8}\eta^{4} + c_{8,2}\xi^{8}\eta^{2} + c_{8,0}\xi^{8} + c_{6,6}\xi^{6}\eta^{6} + c_{6,4}\xi^{6}\eta^{4} + c_{6,2}\xi^{6}\eta^{2} + c_{6,0}\xi^{6} + c_{4,8}\xi^{4}\eta^{8} + c_{4,6}\xi^{4}\eta^{6} + c_{4,4}\xi^{4}\eta^{4} + c_{4,2}\xi^{4}\eta^{2} + c_{4,0}\xi^{4} + c_{2,10}\xi^{2}\eta^{10} + c_{2,8}\xi^{2}\eta^{8} + c_{2,6}\xi^{2}\eta^{6} + c_{2,4}\xi^{2}\eta^{4} + c_{2,2}\xi^{2}\eta^{2} + c_{2,0}\xi^{2} + c_{0,12}\eta^{12} + c_{0,10}\eta^{10} + c_{0,8}\eta^{8} + c_{0,6}\eta^{6} + c_{0,4}\eta^{4} + c_{0,2}\eta^{2} + c_{0,0}.$$
 (38)

Substituting Eq. (38) into the Eq. (27), and equating zero the coefficients of distinct powers of $\xi^r \eta^s$; $r, s \in \mathbb{Z}$, gives a system. On solving this system, we get values as

$$c_{0,0} = \frac{7353680000\alpha_4 c_{10,2}}{1113\alpha_1^6\alpha_3}, c_{0,2} = -\frac{6077833600 c_{10,2}}{371\alpha_1^5}, c_{0,4} = -\frac{6359200\alpha_3 c_{10,2}}{7\alpha_1^4\alpha_4}, c_{0,6} = -\frac{800\alpha_3^2 c_{10,2}}{3\alpha_1^3\alpha_4^2},$$

$$c_{0,8} = \frac{160\alpha_3^3 c_{10,2}}{\alpha_1^2\alpha_4^3}, c_{0,10} = -\frac{10\alpha_3^4 c_{10,2}}{\alpha_1\alpha_4^4}, c_{0,12} = \frac{\alpha_3^5 c_{10,2}}{6\alpha_4^5}, c_{2,0} = \frac{72534400\alpha_4 c_{10,2}}{371\alpha_1^5\alpha_3}, c_{2,2} = \frac{1521600c_{10,2}}{7\alpha_1^4},$$

$$c_{2,4} = -\frac{800\alpha_3 c_{10,2}}{\alpha_1^3\alpha_4}, c_{2,6} = \frac{560\alpha_3^2 c_{10,2}}{\alpha_1^2\alpha_4^2}, c_{2,8} = -\frac{30\alpha_3^3 c_{10,2}}{\alpha_1\alpha_4^3}, c_{2,10} = \frac{\alpha_3^4 c_{10,2}}{\alpha_4^4}, c_{4,0} = -\frac{55200\alpha_4 c_{10,2}}{7\alpha_1^4\alpha_3},$$

$$c_{4,2} = \frac{800c_{10,2}}{\alpha_1^3}, c_{4,4} = \frac{800\alpha_3 c_{10,2}}{\alpha_1^2\alpha_4}, c_{4,6} = -\frac{20\alpha_3^2 c_{10,2}}{\alpha_1\alpha_4^2}, c_{4,8} = \frac{5\alpha_3^3 c_{10,2}}{2\alpha_4^3}, c_{6,0} = \frac{800\alpha_4 c_{10,2}}{3\alpha_1^3\alpha_3},$$

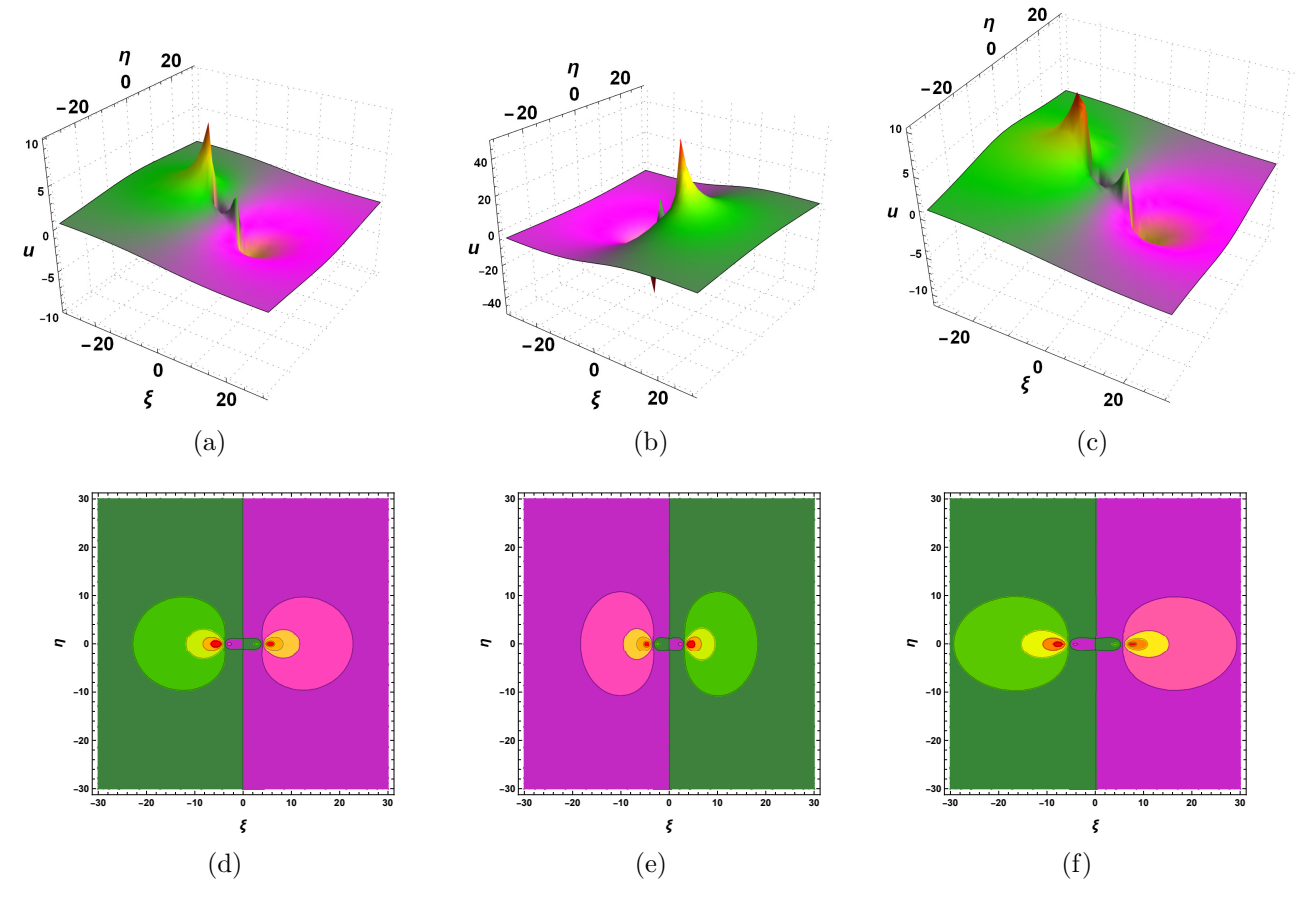


Figure 6: Dynamics of second-order rogue waves for solution (37) in transformed variables ξ and η . (a)-(b) depicts the 3D profiles in $\xi\eta$ -plane, and (d)-(f) shows the contour plots for the (a)-(c).

$$c_{6,2} = \frac{560c_{10,2}}{\alpha_1^2}, c_{6,4} = \frac{20\alpha_3c_{10,2}}{\alpha_1\alpha_4}, c_{6,6} = \frac{10\alpha_3^2c_{10,2}}{3\alpha_4^2}, c_{8,0} = \frac{160\alpha_4c_{10,2}}{\alpha_1^2\alpha_3},$$

$$c_{8,2} = \frac{30c_{10,2}}{\alpha_1}, c_{8,4} = \frac{5\alpha_3c_{10,2}}{2\alpha_4}, c_{10,2} = c_{10,2}, c_{10,0} = \frac{10\alpha_4c_{10,2}}{\alpha_1\alpha_3},$$

$$c_{12,0} = \frac{\alpha_4c_{10,2}}{6\alpha_3},$$

$$(39)$$

with $a_{10,2}$ as an arbitrary parameter. Thus, the equation (29) becomes

$$f = f_3 = \frac{c_{10,2}}{2226} \left(\frac{2226\alpha_3^4\eta^{10}\xi^2}{\alpha_4^4} + \frac{5565\alpha_3^3\eta^8\xi^4}{\alpha_4^3} - \frac{66780\alpha_3^3\eta^8\xi^2}{\alpha_1\alpha_4^3} + \frac{7420\alpha_3^2\eta^6\xi^6}{\alpha_4^2} - \frac{44520\alpha_3^2\eta^6\xi^4}{\alpha_1\alpha_4^2} + \frac{1246560\alpha_3^2\eta^6\xi^2}{\alpha_1^2\alpha_4^2} + \frac{5565\alpha_3\eta^4\xi^8}{\alpha_4} + \frac{44520\alpha_3\eta^4\xi^6}{\alpha_1\alpha_4} + \frac{1780800\alpha_3\eta^4\xi^4}{\alpha_1^2\alpha_4} - \frac{1780800\alpha_3\eta^4\xi^2}{\alpha_1^3\alpha_4} + \frac{66780\eta^2\xi^8}{\alpha_1} + \frac{1246560\eta^2\xi^6}{\alpha_1^2} + \frac{1780800\eta^2\xi^4}{\alpha_1^3} + \frac{483868800\eta^2\xi^2}{\alpha_1^4} + \frac{371\alpha_3^5\eta^{12}}{\alpha_2^5} - \frac{22260\alpha_3^4\eta^{10}}{\alpha_1\alpha_4^4} + \frac{356160\alpha_3^3\eta^8}{\alpha_1^2\alpha_4^3} - \frac{593600\alpha_3^2\eta^6}{\alpha_1^4\alpha_4} - \frac{36467001600\eta^2}{\alpha_1^5} + \frac{371\alpha_4\xi^{12}}{\alpha_3} + \frac{22260\alpha_4\xi^{10}}{\alpha_1\alpha_3} + \frac{356160\alpha_4\xi^8}{\alpha_1^2\alpha_3} + \frac{593600\alpha_4\xi^6}{\alpha_1^2\alpha_3} + \frac{435206400\alpha_4\xi^2}{\alpha_1^5\alpha_3} - \frac{17553600\alpha_4\xi^4}{\alpha_1^4\alpha_3} + \frac{14707360000\alpha_4}{\alpha_1^6\alpha_3} + 2226\eta^2\xi^{10} \right). \quad (40)$$

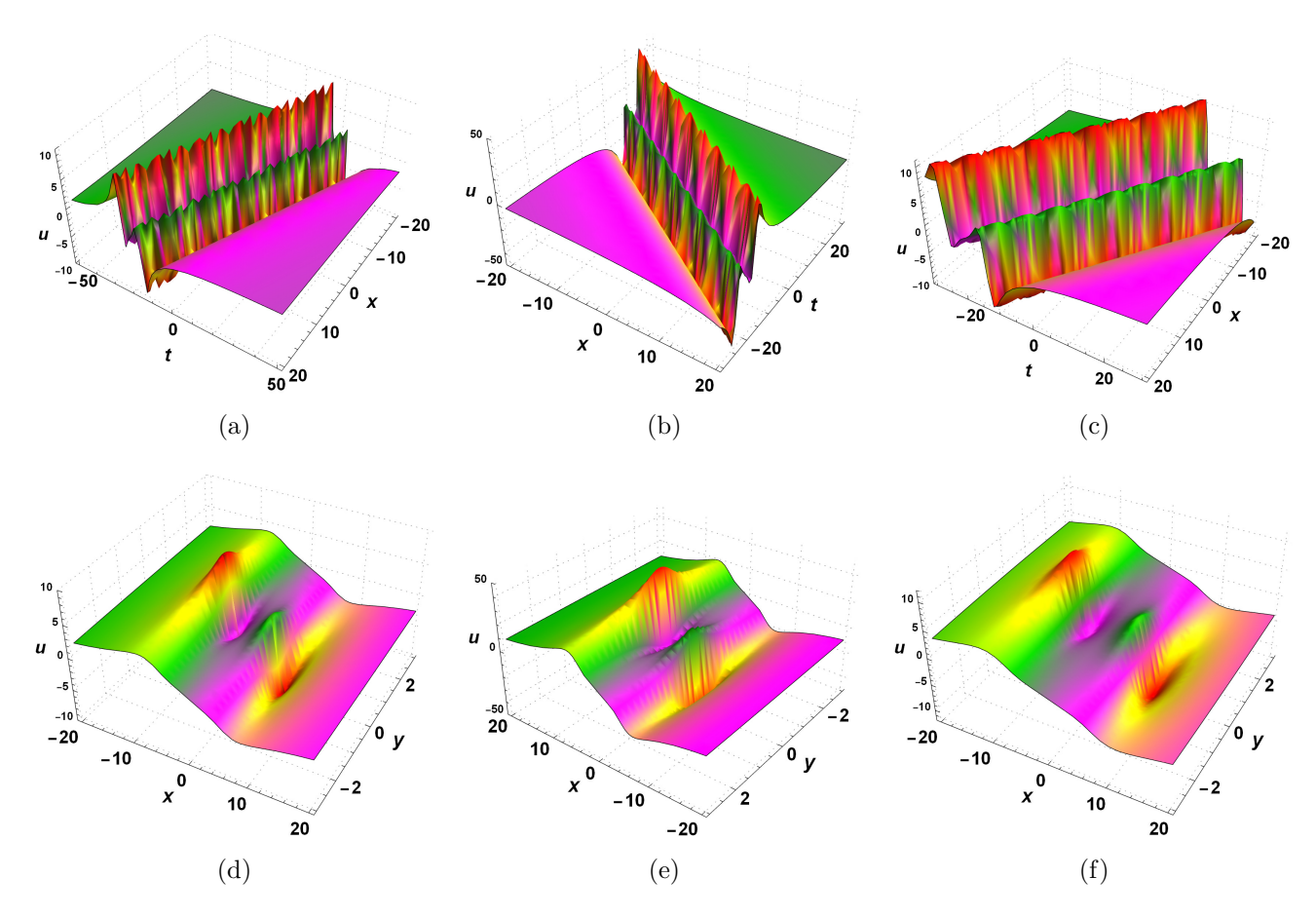


Figure 7: Dynamical profiles of second-order rogue waves for (37) in the starting variables x, y, z, and t under transformed variables $\xi = x + t$ and $\eta = y + z$. (a)-(c) and (d)-(f) depict 3D profiles in xt and xy-planes, respectively.

On having equation (40) into (25), we get a solution of 3^{rd} -order rogue waves as

$$u = u_3 = \frac{6}{\alpha_2} (\log f_3)_{\xi}. \tag{41}$$

5 Results and findings

The proposed KdV-type evolution equation showed the completely integrable using Painlevé analysis. Thus, it has soliton solutions for kink type with the Hirota bilinear technique. The first-order soliton solution generated the single kink-soliton, and the second and third-order soliton solutions showed the interaction solutions for two and three kink-solitons with an appropriate selection of parameters. After that, the rogue wave solutions for the investigated equation utilize a direct symbolic approach. The first-order rogue solution generated a single rogue wave solution, and second and third-order rogue solutions gave the interactions of rogue waves. The dynamics of rogue wave solutions have been shown in transformed variables ξ, η , and in the starting variables x, y, z, t in $\xi \eta, xt$, and xy planes. In this context, the dynamical findings are as follows:

- Figure-1 show the one solitons of kink-type, and the solitons (a) and (c) are propagating to the right, while (b) is propagating to the left of x-axis. The illustrated kink-solitons have the parameter values

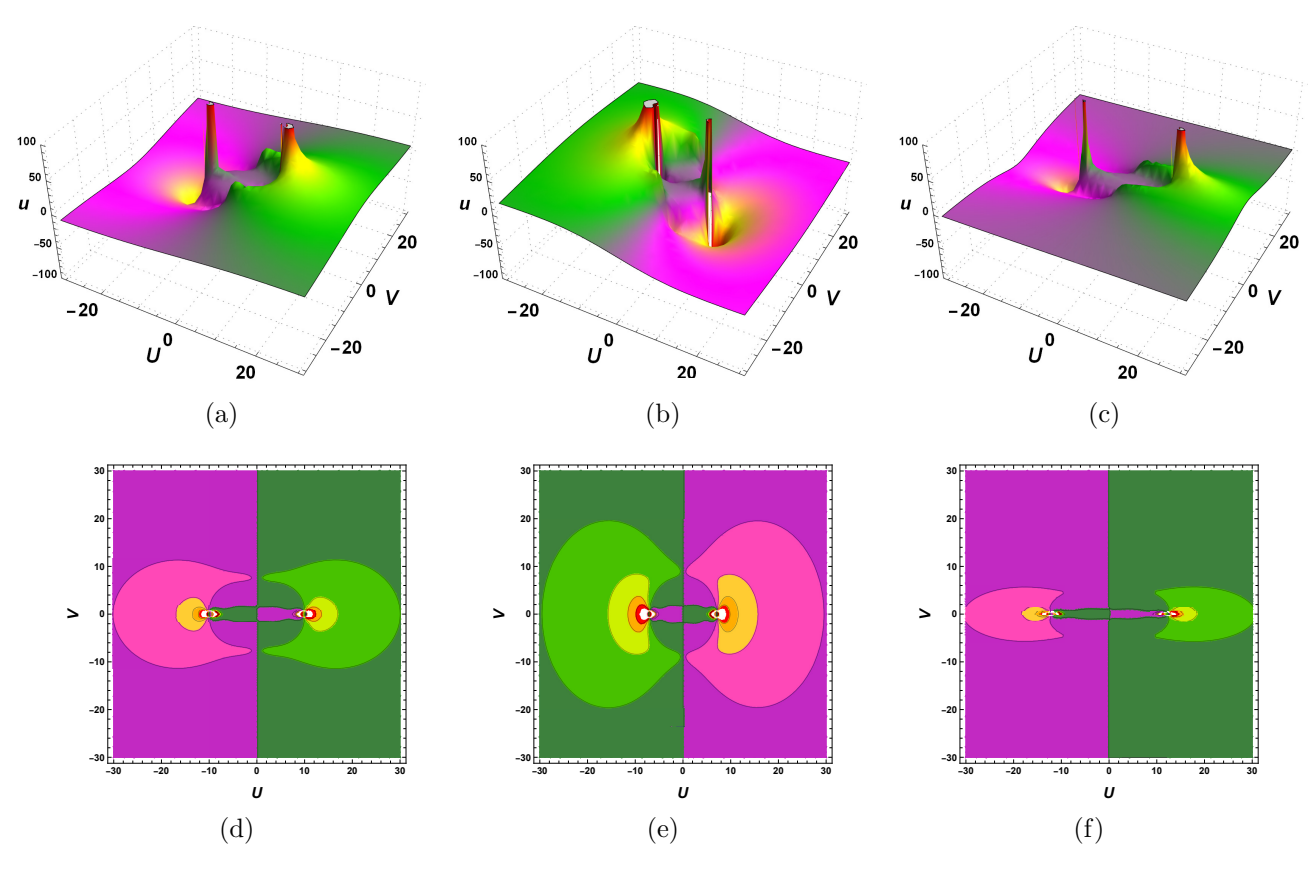


Figure 8: Dynamics of third-order rogue waves for solution (37) in transformed variables ξ and η . (a)-(b) depicts the 3D profiles in $\xi\eta$ -plane, and (d)-(f) shows the contour plots for the (a)-(c).

as (a)
$$p_1 = q_1 = r_1 = 1$$
, $\alpha_i = 1, 1 \le i \le 4$; (b) $p_1 = 1, q_1 = -0.3, r_1 = \alpha_1 = 1, \alpha_2 = -1, \alpha_3 = \alpha_4 = 1$; and (c) $p_1 = 1, q_1 = 0.4, r_1 = 0, \alpha_1 = 1, \alpha_2 = -1, \alpha_3 = \alpha_4 = 1$.

- In Figure-2, we show the two-soliton solutions of kink-types. The dynamics depicts the interactions of the two kink-type soliton solutions with chosen parameter values. The showed kink-solitons have the parameter values as (a) $p_1 = 1$, $p_2 = -1$, $q_1 = 0.5 = q_2$, $r_1 = 0.5 = r_2$, $q_1 = 1$, $q_2 = -1$, $q_3 = q_4 = 1$; (b) $p_1 = 1$, $p_2 = -1$, $q_1 = 0.7$, $q_2 = 0.5$, $q_2 = 0.5$, $q_3 = 0.5$
- Figure-3 depict the three-soliton solutions of kink-types. The dynamics depicts the interactions of the three kink-type soliton solutions with chosen parameters. The showed kink-solitons have the parameter values as (a) $p_1 = 1, p_2 = -1 = p_3, q_1 = 0.7, q_2 = 0.5, q_3 = 0.6, r_1 = 0.5 = r_2 = r_3, \alpha_1 = 1, \alpha_2 = -1, \alpha_3 = \alpha_4 = 1$; (b) $p_1 = 1, p_2 = -1 = p_3, q_1 = 1.5, q_2 = 0.5 = q_3, r_1 = 0.5 = r_2, r_3 = 0.6, \alpha_1 = 1, \alpha_2 = -1, \alpha_3 = \alpha_4 = 1$; and (c) $p_1 = -1, p_2 = 1, p_3 = -1, q_1 = 0.7, q_2 = 0.5, q_3 = 0.6, r_1 = 0.5 = r_2 = r_3, \alpha_1 = 1, \alpha_2 = -1, \alpha_3 = \alpha_4 = 1$.
- In Figure-4 and 5, we illustrate the rogue waves of first order which depict the single rogues with singularities at $\xi = \eta = 0$. For all three plots in Figure-4, positive and negative direction of ξ shows the bright and the dark part of the rogue wave dynamics. Figure-5 depicts the single rogue wave structures in the original variables x, y, z, t. (a)-(c) shows the periodic behavior w.r.t. time variable in xt-plane with y = z = 0 and (d)-(f) shows the single rogue waves in xy-plane with z = t = 0. The showed single rogue waves for both figures have the parameter values as (a) $\alpha_2 = 5$, $\alpha_3 = \alpha_4 = 1$; (b)

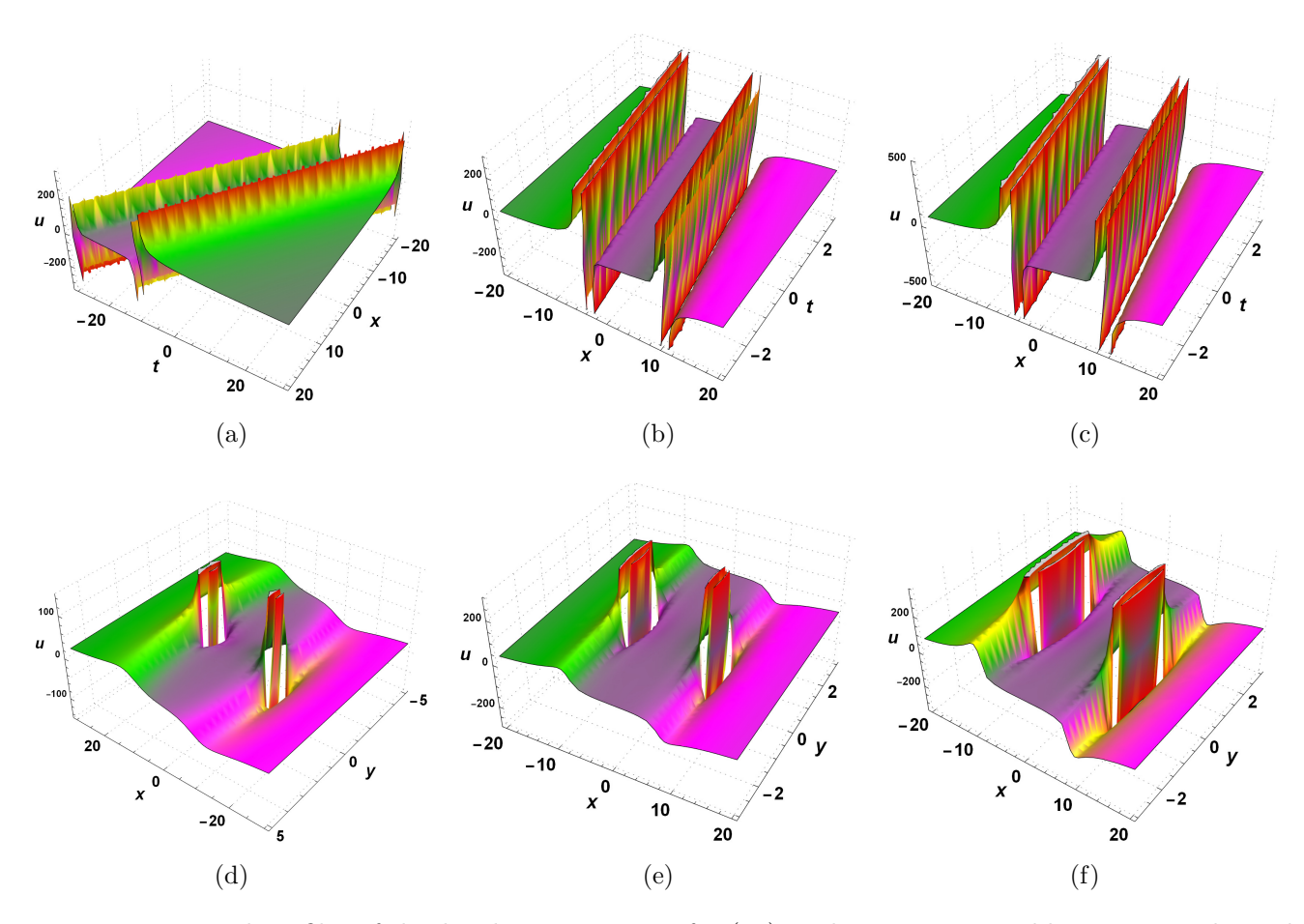


Figure 9: Dynamical profiles of third-order rogue waves for (41) in the starting variables x, y, z, and t under transformed variables $\xi = x + t$ and $\eta = y + z$. (a)-(c) and (d)-(f) depict 3D profiles in xt and xy-planes, respectively.

$$\alpha_2 = 10, \alpha_3 = 5, \alpha_4 = 1; \text{ and } (\mathbf{c}) \ \alpha_2 = 1, \alpha_3 = 3, \alpha_4 = 5.$$

- Figure-6 and 7 depict the rogue waves of second order which show the two rogues having dominating nature of extreme rogue waves to the smaller rogues. For all three graphs in Figure-6, the two rogues intersect at $\xi = \eta = 0$ with having their bight and dark parts. Figure-7 shows the two rogue wave structures in the original variables x, y, z, t. (a)-(c) shows the periodic nature w.r.t. time variable, in xt-plane with y = z = 0 and (d)-(f) shows the two rogue waves in xy-plane with z = t = 0. The showed second-order rogue waves for both figures have the parameter values as (a) $\alpha_1 = 0.2$, $\alpha_2 = -0.8$, $\alpha_3 = \alpha_4 = 1$; (b) $\alpha_1 = 0.3$, $\alpha_2 = 0.2$, $\alpha_3 = 1$, $\alpha_4 = 2$; and (c) $\alpha_1 = 0.1$, $\alpha_2 = -0.5$, $\alpha_3 = -3$, $\alpha_4 = -2$.
- In Figure-8 and 9, we illustrate the third-order rogue waves that depict the four rogue waves having dominating nature of extreme rogue waves to the smaller rogues. For all three plots in Figure-8, the four rogues depict the intersections having their bight and dark parts. Figure-9 shows the four rogue wave structures in the original variables x, y, z, t. (a)-(c) shows the periodicity w.r.t. time variable in xt-plane with y=z=0 and (d)-(f) shows the four rogue waves in xy-plane with z=t=0. The showed third-order rogue waves for both figures have the parameter values as (a) $\alpha_1=-0.3, \alpha_2=0.1, \alpha_3=-0.7, \alpha_4=-0.5$; (b) $\alpha_1=-0.6, \alpha_2=-0.1, \alpha_3=0.1, \alpha_4=0.2$; and (c) $\alpha_1=-0.5, \alpha_2=-0.05, \alpha_3=0.4, \alpha_4=0.1$.

6 Conclusions

This research article proposed a new Painlevé integrable (3+1)-dimensional generalized nonlinear KdV-type equation. The Painlevé analysis confirmed the complete integrability. We constructed the bilinear form in Hirota's *D*-operators with the Cole-Hopf transformation of the auxiliary function. Using the Hirota bilinear technique, the soliton solutions for the investigated equation were formed in the third order, showing their type as kinks, and the second and third orders have the interactions of kink-solitons. After that, we constructed the rogue wave solutions for the proposed equation utilizing the direct symbolic approach with a logarithmic transformation to construct the bilinear form. We obtained the rogue wave solutions, and in second and third-order solutions, the waves showed the dominating nature of large rogues over the smaller rogues. Using the symbolic software *Mathematica*, we have shown the dynamics for the higher-order solitons and rogue waves with appropriate parameter values. Dynamics for the rogue waves were studied in both transformed and starting variables, which helps to understand the nature of rogues in starting variables concerning the transformed variables.

The proposed equation generalizes the well-known equations having applications in nonlinear sciences and soliton theory. Thus, this equation can explore water wave solutions such as lumps, breathers, and other periodic waves. We studied this equation using two methods for soliton and rogue wave solutions, so different techniques can be used to construct several other solutions in nonlinear fields. Future work will focus on extending the analysis to other high-dimensional nonlinear systems and exploring potential applications in real-world scenarios such as fluid dynamics, fiber optics, and atmospheric science. This research could provide valuable insights into wave behavior in extreme environments, paving the way for new advances in nonlinear sciences and mathematical physics.

Declarations

Ethics approval and consent to participate

This is not applicable.

Competing interests

According to the authors, there are no conflicts of interest.

Authors' contributions

All the authors have agreed and given their consent for the publication of this research paper.

Data availability statement

The data that supports the findings of the study are available in the article.

References

- [1] Xing Lü, Si-Jia Chen: N-soliton solutions and associated integrability for a novel (2+1)-dimensional generalized KdV equation, Chaos Soli Fract. **169**, 113291, (2023)
- [2] Kumar, S., Mohan, B.: A study of multi-soliton solutions, breather, lumps, and their interactions for Kadomtsev- Petviashvili equation with variable time coefficient using Hirota method. Phys. Scr. **96**(12), 125255 (2021)

- [3] Wazwaz, A.M., Hammad, M.A., El-Tantawy,S.A.: Bright and dark optical solitons for (3 + 1)dimensional hyperbolic nonlinear Schrödinger equation using a variety of distinct schemes, Optik, 270, 170043, (2022)
- [4] Kumar, S., Mohan, B., Kumar, R.: Lump, soliton, and interaction solutions to a generalized two-mode higher-order nonlinear evolution equation in plasma physics. Nonlinear Dyn, **110**, 693–704, (2022)
- [5] Shen, Y., Tian, B., Zhou, T.Y., Gao, X.T.: Shallow water wave studies on a (2+1)-dimensional Hirota-Satsuma-Ito system: X-type soliton, resonant Y-type soliton and hybrid solutions, Chaos Soli Fract. 157, 111861, (2022)
- [6] Seadawy, A.R., Ali, K.K., Nuruddeen, R.I.: A variety of soliton solutions for the fractional Wazwaz-Benjamin-Bona-Mahony equations, Results in Physics, 12, 2234-2241, (2019)
- [7] Seadawy, A.R., Alsaedi, B.: Contraction of variational principle and optical soliton solutions for two models of nonlinear Schrodinger equation with polynomial law nonlinearity, AIMS Mathematics, 9(3), 6336-6367, (2024)
- [8] Li L., Xie Y.: Rogue wave solutions of the generalized (3+1)-dimensional Kadomtsev-Petviashvili equation. Chaos Soli Fract. **147**, 110935, (2021)
- [9] Kumar, S., Mohan, B.: A novel analysis of Cole-Hopf transformations in different dimensions, solitons, and rogue waves for a (2+1)-dimensional shallow water wave equation of ion-acoustic waves in plasmas. Physics of Fluids, **35**(12),127128 (2023)
- [10] Li, L., Xie, Y., Mei, L.: Multiple-order rogue waves for the generalized (2+1)-dimensional Kadomt-sev-Petviashvili equation, Applied Mathematics Letters, 117, 107079, (2021)
- [11] Abdeljabbar, A., Hossen, M.B., Roshid, HO. et al:. Interactions of rogue and solitary wave solutions to the (2+1)-D generalized Camassa-Holm-KP equation, Nonlinear Dyn, **110**, 3671-3683 (2022)
- [12] Hossen, M.B., Roshid, HO, Ali, M.Z.: Characteristics of the solitary waves and rogue waves with interaction phenomena in a (2+1)-dimensional Breaking Soliton equation, Physics Letters A, **382**(19), 1268-1274, (2018)
- [13] Elboree, M.K.: Higher order rogue waves for the (3 + 1)-dimensional Jimbo-Miwa equation, International Journal of Nonlinear Sciences and Numerical Simulation, **23**, 7-8, (2022)
- [14] Mohan, B., Kumar, S., Kumar, R. Higher-order rogue waves and dispersive solitons of a novel P-type (3+1)-D evolution equation in soliton theory and nonlinear waves. Nonlinear Dyn. **111**, 20275–20288 (2023)
- [15] Liu, W., Zhang, Y.: Multiple rogue wave solutions for a (3+1)-dimensional Hirota bilinear equation. Appl. Math. Lett. **98**, 184–190 (2019)
- [16] Tang, Y., Ma, W.X., Xu, W., Gao, L.: Wronskian determinant solutions of the (3+1)-dimensional Jimbo–Miwa equation, Applied Mathematics and Computation, **217**(21), 8722-8730 (2011)
- [17] He, C., Tang, Y., Ma, W. et al.: Interaction phenomena between a lump and other multi-solitons for the -dimensional BLMP and Ito equations. Nonlinear Dyn. **95**, 29–42 (2019)
- [18] Alam, M.N., Tunç, C.: New solitary wave structures to the (2 + 1)-dimensional KD and KP equations with spatio-temporal dispersion, Journal of King Saud University Science, 32(8), 3400-3409 (2020)

- [19] Hirota R.: The direct method in soliton theory. Cambridge: Cambridge University Press, (2004).
- [20] Kumar, S., Mohan, B., Kumar, A.: Generalized fifth-order nonlinear evolution equation for the Sawada-Kotera, Lax, and Caudrey-Dodd-Gibbon equations in plasma physics: Painlevé analysis and multi-soliton solutions, Phys. Scr., 97, 035201, (2022)
- [21] Wazwaz, A.M.: Painlevé integrability and lump solutions for two extended (3 + 1)- and (2 + 1)-dimensional Kadomtsev–Petviashvili equations, Nonlinear Dyn, 111, 3623–3632 (2023)
- [22] Singh, S., Ray, S.S.: The Painlevé integrability and abundant analytical solutions for the potential Kadomtsev–Petviashvili (pKP) type coupled system with variable coefficients arising in nonlinear physics, Chaos Soli Fract. 175(1), 113947, (2023)
- [23] Seadawy A.R.: Stability analysis for Zakharov–Kuznetsov equation of weakly nonlinear ion-acoustic waves in a plasma, Comp. Math. with App., **67**(1), 172-180, (2014)
- [24] Seadawy, A.R., Rizvi, S.T.R., Ali, I. et al.: Conservation laws, optical molecules, modulation instability and Painlevé analysis for the Chen–Lee–Liu model, Opt Quant Electron 53, 172, (2021)
- [25] Mohan, B., Kumar, S.: Rogue-wave structures for a generalized (3+1)-dimensional nonlinear wave equation in liquid with gas bubbles, Physica Scripta, 99, 105291, (2024)
- [26] Hossen, M.B., Roshid, HO, Ali, M.Z., Rezazadeh, H.: Novel dynamical behaviors of interaction solutions of the (3 + 1)-dimensional generalized B-type Kadomtsev-Petviashvili model, Phys. Scr., **96**, 125236, (2021)
- [27] Hossen, M.B., Roshid, HO, Ali, M.Z.: Multi-soliton, breathers, lumps and interaction solution to the (2+1)-dimensional asymmetric Nizhnik-Novikov-Veselov equation, Heliyon, **5**(10), e02548, (2019)
- [28] Mohan, B., Kumar, S.: Generalization and analytic exploration of soliton solutions for nonlinear evolution equations via a novel symbolic approach in fluids and nonlinear sciences, Chinese Journal of Physics, 92, 10-21, (2024)
- [29] Seadawy, A.R., Arshad, M., Lu, D.: The weakly nonlinear wave propagation theory for the Kelvin-Helmholtz instability in magnetohydrodynamics flows, Chaos Soli Fract., 139, 110141, (2020)
- [30] Jhangeer, A., Rezazadeh, H., Seadawy, A.: A study of travelling, periodic, quasiperiodic and chaotic structures of perturbed Fokas-Lenells model. Pramana J Phys. 95, 41 (2021)
- [31] Seadawy, A.R., Alsaedi, B.A.: Soliton solutions of nonlinear Schrödinger dynamical equation with exotic law nonlinearity by variational principle method. Opt Quant Electron, **56**, 700 (2024)
- [32] Guan X., Liu W., Zhou, Q. et al.: Darboux transformation and analytic solutions for a generalized super-NLS-mKdV equation. Nonlinear Dyn. 98, 1491–1500 (2019)
- [33] Lan, Z.Z.: Rogue wave solutions for a higher-order nonlinear Schrödinger equation in an optical fiber, Applied Mathematics Letters **107**, 106382, (2020)
- [34] Wang, X., Wei, J.: Three types of Darboux transformation and general soliton solutions for the space-shifted nonlocal PT symmetric nonlinear Schrödinger equation, Applied Mathematics Letters, 130, 107998, (2022)
- [35] Hereman W., Nuseir A.: Symbolic methods to construct exact solutions of nonlinear partial differential equations. Math Comput Simul, 43, 13–27 (1997)

- [36] Wazwaz, A.M.: Multiple soliton solutions for a (2+1)-dimensional integrable KdV6 equation. Commun. Nonlinear Sci. Numer. Simul. 15, 1466–1472 (2010).
- [37] Huang Z.R., Tian B., Zhen H.L. et al.: Bäcklund transformations and soliton solutions for a (3+1)-dimensional B-type Kadomtsev-Petviashvili equation in fluid dynamics. Nonlinear Dyn. 80, 1-7 (2015)
- [38] Yan, X.W., Tian, S.F., Dong, M.J. et al.: Bäcklund transformation, rogue wave solutions and interaction phenomena for a (3+1)(3+1)-dimensional B-type Kadomtsev-Petviashvili-Boussinesq equation. Nonlinear Dyn. 92, 709–720 (2018)
- [39] Zhang, R., Bilige, S. Chaolu, T.: Fractal Solitons, Arbitrary Function Solutions, Exact Periodic Wave and Breathers for a Nonlinear Partial Differential Equation by Using Bilinear Neural Network Method. J Syst Sci Complex 34, 122–139 (2021)
- [40] Zhang, RF., Li, MC., Cherraf, A. et al.: The interference wave and the bright and dark soliton for two integro-differential equation by using BNNM. Nonlinear Dyn. 111, 8637–8646 (2023)
- [41] Liu, F.Y., Gao, Y.T. et al.: Painlevé analysis, Lie group analysis and soliton-cnoidal, resonant, hyper-bolic function and rational solutions for the modified Korteweg-de Vries-Calogero-Bogoyavlenskii-Schiff equation in fluid mechanics/plasma physics, Chaos Soli Fract. 144, 110559 (2021)
- [42] Hamid, I., Kumar, S.: Symbolic computation and Novel solitons, traveling waves and soliton-like solutions for the highly nonlinear (2+1)-dimensional Schrödinger equation in the anomalous dispersion regime via newly proposed modified approach. Opt Quant Electron, **55**, 755, (2023)
- [43] Kumar, S., Kumar, A., Mohan, B.: Evolutionary dynamics of solitary wave profiles and abundant analytical solutions to a (3+1)-dimensional burgers system in ocean physics and hydrodynamics, Journal of Ocean Engineering and Science, 8(1), 1-14, (2023)
- [44] Wazwaz A.M.: The Hirota's direct method for multiple soliton solutions for three model equations of shallow water waves. Appl. Math. Comput. **201**, 489–503 (2008)
- [45] Yang, L., Gao, B.: The nondegenerate solitons solutions for the generalized coupled higher-order non-linear Schrödinger equations with variable coefficients via the Hirota bilinear method, Chaos Soli Fract. 184, 115009, (2024)
- [46] Kumar, S., Mohan, B.: A generalized nonlinear fifth-order KdV-type equation with multiple soliton solutions: Painlevé analysis and Hirota Bilinear technique, Phys. Scr. **97**(12), 125214 (2022)
- [47] Jiang Y., Tian B., Wang P. et al.: Bilinear form and soliton interactions for the modified Kadomt-sev-Petviashvili equation in fluid dynamics and plasma physics. Nonlinear Dyn. 73, 1343–1352 (2013)
- [48] Weiss J, Tabor M, Carnevale G. The Painlevé property for partial differential equations. J. Math. Phys. 24, 522–526 (1983)
- [49] Kumar, S., Mohan, B. A direct symbolic computation of center-controlled rogue waves to a new Painlevé-integrable (3+1)-D generalized nonlinear evolution equation in plasmas. Nonlinear Dyn, 111:16395–16405, (2023)
- [50] Yang, X., Zhang, Z., Wazwaz A.M., Wang, Z.: A direct method for generating rogue wave solutions to the (3+1)-dimensional Korteweg-de Vries Benjamin-Bona-Mahony equation, Physics Letters A 449, 128355, (2022)